Significant enhancement of group delay in electromagnetically induced transparency with a spatially partially coherent coupling field

You-Lin Chuang ⓞ*

Physics Division, National Center for Theoretical Sciences, Taipei 10617, Taiwan

The slow light propagation effect in electromagnetically induced transparency with a spatial partially coherent coupling field has been studied. We find that the group velocity of the probe beam can be significantly reduced when the spatial coherence of the coupling field decreases. It shows that the group delay of the probe beam can achieve about 10 times that of the fully coherent case. This work shows the effect of spatial coherence of the coupling field in a coherent atomic medium and provides a slow-light mechanism in optical coherence systems.

I. INTRODUCTION

Electromagnetically induced transparency (EIT) [1,2] is a quantum interference phenomenon which has been observed in various physical systems [3,4]. Some novel properties of EIT, such as ultralow absorption [5], steep dispersion [6], slow light effect [7], and light storage [8,9], have been proposed to apply in some devices [10]. In the recent decade, the studies on strong interactions between Rydberg atoms based on EIT have been paid great attention [11]. With the controllable conditions in practical experiments, EIT has promising potential in the progress of quantum computers and communications. In addition to the properties mentioned above, EIT can be used to preserve the quantum state of light, ensuring the intactness of quantum squeezing of input fields under certain conditions [12]. Besides, EIT can play an entangler, which can create quantum entanglement between the two interacting fields [13]. Its simple configuration and ease of manipulation in experiments make EIT an ideal system not only for applications but also for fundamental research. It is no doubt that EIT is a great candidate to help us study new physical phenomena.

In conventional EIT experiments, people use laser light sources which have great temporal and spatial coherence, and one can obtain good matching results between experimental observations and theoretical simulations. However, more general studies of the interactions between the partially coherent light source and resonant atomic media are still missing. The degree of coherence provides an extra degree of freedom to study the physics of atom-light interactions and field propagation in the media, and it has no counterparts in fully coherent light, which has a coherence length much larger than 1. On the other hand, many important applications of partially coherent beams have been widely studied, such as microdensitometry [14], holography [15], lithography [16], free space optical communications [17], ghost imaging [18], and plasmonics [19].

In recent decades, some interesting properties of EIT in the quantum domain have been intensely investigated. The

quantum noises and correlations can be transferred between the two interacting fields via the atomic coherent process [20]. With a similar process, it is natural to consider the transfer process for the stochastic properties of the partially coherent lights in an EIT system. It is evident that the connection between partially coherent light sources and quantum coherence in atomic media provides a different avenue to study light-matter interactions.

Here we are interested in the case of a spatially partially coherent light source, which has an extra physical degree of freedom that never exists in the fully coherent light case. In order to quantitatively study the effect of the spatially partially coherent light in EIT, we consider how the slow light changes in EIT, i.e., group delay of the probe beam under the different spatial coherence degrees of the coupling field. In the fully coherent case, the group delay of the probe beam is inversely proportional to the intensity of the coupling field [21]. However, in the spatially partially coherent case, the intensity of the coupling field in the EIT medium would be affected by the initial coherence degree, so the group delay of the probe beam is also dependent on the initial spatial coherence of the coupling field. According to the concept, one can expect that the slow light propagation, as well as the absorption and dispersion relation, is essentially related to the coherence degree of the coupling field. This is the main idea of this work.

The organization of this paper is as follows. In Sec. II, we start from a fundamental formula of the EIT system and introduce the spatial coherence degree. A general expression for the probe beam pulse propagation under the spatially partially coherent coupling field is derived. In Sec. III, we will show our results, comparing the two cases of full coherence and partial coherence. Some discussions and physical interpretations are also included in Sec. III. Finally, a brief conclusion is given in Sec. IV.

II. THEORETICAL MODEL

Let us consider a type Λ-type EIT configuration, which has two lower states labeled by |1⟩ and |2⟩ and one excited state |3⟩. The two interacting fields, probe and coupling, couple to
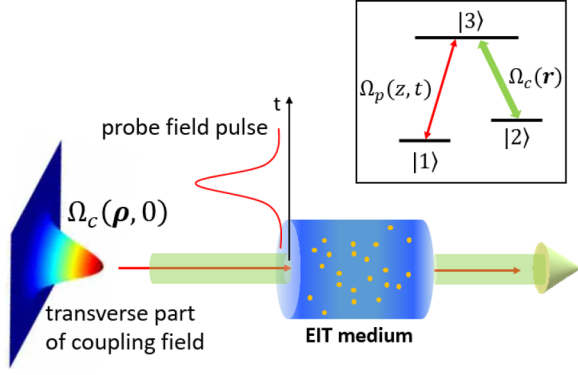
─────────
*chuang_youlin@gapp.nthu.edu.tw

FIG. 1. The EIT setup. Two light fields, the probe field (thin red arrow) and the coupling field (thick green arrow), interact with an atomic ensemble. The atomic configuration is shown in the inset

the dipole transitions from $|1\rangle \to |3\rangle$ and $|2\rangle \to |3\rangle$, respectively. The EIT configuration is shown in the insert of Fig. 1. Under the EIT condition, the intensity of the probe beam is much weaker than that of the coupling field; therefore, one has a good approximation to consider that most populations of atoms stay on the ground state $|1\rangle$. Since only the first-order atomic coherence terms are important, we can write the equations of motion for the first-order atomic density matrix elements [22] as

$$\frac{\partial}{\partial t}\rho_{31} \simeq -(\gamma_{31} - i\Delta_p)\rho_{31} + \frac{i}{2}\Omega_p(\mathbf{r}, t) + \frac{i}{2}\Omega_c(\mathbf{r})\rho_{21},$$
$$(1)$$

$$\frac{\partial}{\partial t}\rho_{21} \simeq -(\gamma_{21} - i\delta_p)\rho_{21} + \frac{i}{2}\Omega_c^*(\mathbf{r})\rho_{31}, \qquad (2)$$

where γ_{31} and γ_{21} are the dephasing rates of ρ_{31} and ρ_{21}. Δ_p and δ_p are the one- and two- photon detunings, and Ω_p and Ω_c are the Rabi frequencies of the probe and coupling fields, respectively. The definition of the Rabi frequency of a field is $\Omega \equiv \mu E/\hbar$, where μ is the electric dipole moment of the corresponding dipole transition, and E is the electric field amplitude. It is noticed that the two Rabi frequencies $\Omega_p(\mathbf{r}, t)$ and $\Omega_c(\mathbf{r})$ are spatial dependent. Here $\mathbf{r} \equiv (\boldsymbol{\rho}, z)$ stands for the transverse part $\boldsymbol{\rho}$ and the longitudinal part z.

On the other hand, the field propagation equation of the probe beam is governed by the Maxwell-Schrödinger equation, that is,

$$\left[\left(\frac{\partial}{\partial z} + \frac{1}{c}\frac{\partial}{\partial t}\right) + \frac{1}{2ik}\nabla_\perp^2\right]\Omega_p = i\frac{\Gamma\alpha}{2L}\rho_{31}, \qquad (3)$$

where $\nabla_\perp^2 \equiv \partial_x^2 + \partial_y^2$ is the transverse Laplacian operator. α is the optical density of the EIT atomic medium. Γ is the excited-state spontaneous emission rate, and its value $\Gamma = 2\pi \times 6$ MHz in the ^{87}Rb atom. L is the medium length, and c is the speed of light. It is clear to see that the probe beam propagation equation given in Eq. (3) depends on the atomic coherence term ρ_{31} and essentially couples to Eqs. (1) and (2).

Compared with the probe beam, we assume that the coupling field is freely propagating through the EIT medium because the contribution of the corresponding atomic dipole source term ρ_{32} is negligible. However, the transverse effect of the coupling field is taken into account in order to introduce

the effect of spatial coherence into our system. Under paraxial approximation, the coupling field solution is given as

$$E_c(\boldsymbol{\rho}, z) = -\frac{ik}{2\pi z}e^{ikz}\iint_{\text{IP}} d^2\boldsymbol{\rho}' \, E_c(\boldsymbol{\rho}', 0)\exp\left[\frac{ik}{2z}(\boldsymbol{\rho} - \boldsymbol{\rho}')^2\right].$$
$$(4)$$

In Eq. (4), the coupling field amplitude at $z = z$ can be determined by its amplitude in the incident plane (IP) at $z = 0$. Since we consider the stochastic behaviors in transverse of the coupling beam, it is relevant to obtain the statistical average of the field correlations. Therefore, the statistical average of the coupling field can be directly calculated by Eq. (4). It shows

$$\langle|E_c(\boldsymbol{\rho}, z)|^2\rangle = \left(\frac{k}{2\pi z}\right)^2\iint_{\text{IP}} d^2\boldsymbol{\rho}' \iint_{\text{IP}} d^2\boldsymbol{\rho}'' W(\boldsymbol{\rho}', \boldsymbol{\rho}'', 0)$$
$$\times \exp\left\{\frac{ik}{2z}[(\boldsymbol{\rho} - \boldsymbol{\rho}'')^2 - (\boldsymbol{\rho} - \boldsymbol{\rho}')^2]\right\}, \quad (5)$$

where $W(\boldsymbol{\rho}', \boldsymbol{\rho}'', 0) \equiv \langle E_c^*(\boldsymbol{\rho}', 0)E_c(\boldsymbol{\rho}'', 0)\rangle$ is the cross spectral density (CSD) of the input coupling field. In Eq. (5), one can find that the coupling field intensity at z essentially depends on the CSD at the incident plane. Here we consider the coupling beam generated by the electromagnetic Gaussian Schell-model source [23], for which the CSD can be expressed by

$$W(\boldsymbol{\rho_1}, \boldsymbol{\rho_2}) = \sqrt{S(\boldsymbol{\rho_1})}\sqrt{S(\boldsymbol{\rho_2})}\,\mu(\boldsymbol{\rho_2} - \boldsymbol{\rho_1}), \qquad (6)$$

in which

$$S(\boldsymbol{\rho}) = A^2 \exp(-\boldsymbol{\rho}^2/2\sigma^2), \qquad (7)$$

$$\mu(\boldsymbol{\rho_2} - \boldsymbol{\rho_1}) = \exp\left[-\frac{(\boldsymbol{\rho_1} - \boldsymbol{\rho_2})^2}{2\delta^2}\right], \qquad (8)$$

where A, σ, and δ are all positive quantities, and they are independent of position. A^2 is proportional to the coupling beam intensity. σ and δ are the beam width and the coherence length of the coupling beam, respectively.

According to Eqs. (5)–(8), we can obtain the statistical average of the coupling field intensity at z as

$$\langle|E_c(\boldsymbol{\rho}, z)|^2\rangle = A^2 \frac{1}{\beta^2}\exp\left(-\frac{\boldsymbol{\rho}^2}{2\sigma^2\beta^2}\right), \qquad (9)$$

and

$$\beta^2 \equiv 1 + \frac{z^2}{4k^2\sigma^4}\left(1 + \frac{4}{q^2}\right), \qquad (10)$$

where $q \equiv \delta/\sigma$ is called the degree of global coherence of the source [24,25], which is the ratio between the coherence length and the beam width of an optical beam. When $q \gg 1$, the source is considered as coherent in the global sense, while $q \ll 1$, the source is treated as incoherent in the global sense. The coherence length δ can be achieved to the order of μm in practical experiments [26–28]. The two parameters, δ and σ, are two independent quantities, and it is possible to achieve a small value of q by increasing the beam width. The coherence length in experiments ranging from 27 to 112 μm can be achieved [27]. One can use suitable beam width σ for the corresponding δ, so that $q = 0.002$ is achievable in practical experiments.
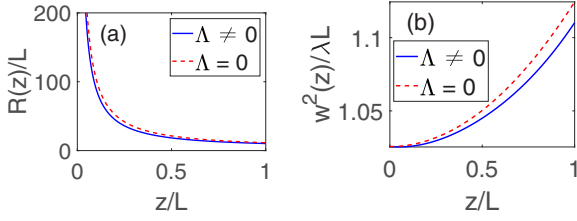
FIG. 2. The curvature $R(z)$ and width $w^2(z)$ of the Gaussian beam. The blue curves are the results when $\Lambda \neq 0$, while the red dashed curves are the case with $\Lambda = 0$. The parameters we used here are $\sigma = 1$ mm, $\sigma_{\text{probe}} = 0.2\sigma$, $L = 5$ cm, $\Delta_p = 0 = \delta_p$, $\Omega_0 = 0.7\Gamma$, $\lambda = 780$ nm, $\tau = 40(1/\Gamma)$, $\omega = (1/40)\Gamma$, and $q = 0.002$.

The propagation solution of probe field can be found by using the Fourier transform to the coupled equations given by Eqs. (1), (2), and (3). Then one can obtain the following equation:

$$\left(\frac{\partial}{\partial z} + \frac{1}{2ik} \nabla_{\perp}^2 \right) \tilde{\Omega}_p(z, \boldsymbol{\rho}, \omega) = -\Lambda(z, \boldsymbol{\rho}, \omega) \tilde{\Omega}_p(z, \boldsymbol{\rho}, \omega),$$
(11)

where

$$\Lambda(z, \boldsymbol{\rho}, \omega) = \frac{(\Gamma \alpha / 4L)(\tilde{\gamma}_{21} - i\omega)}{(\tilde{\gamma}_{31} - i\omega)(\tilde{\gamma}_{21} - i\omega) + \langle |\Omega_c(\boldsymbol{\rho}, z)|^2 \rangle / 4} - i \frac{\omega}{c}.$$
(12)

Here we can find the statistical average of coupling field Rabi frequency $\langle |\Omega_c(\boldsymbol{\rho}, z)|^2 \rangle$ in the probe field equation. It can directly obtain $\langle |\Omega_c(\boldsymbol{\rho}, z)|^2 \rangle$ in Eq. (12) from Eqs. (9) and (10). It is

$$\langle |\Omega_c(\boldsymbol{\rho}, z)|^2 \rangle = |\Omega_0|^2 \frac{1}{\beta^2} \exp\left(-\frac{\boldsymbol{\rho}^2}{2\sigma^2 \beta^2} \right),$$
(13)

where $\Omega_0 \equiv \mu_{32} A / \hbar$ in Eq. (13) is the Rabi frequency of input coupling field in the center of the incident plane. Besides, in Eq. (12) we have used the replacements that $\tilde{\gamma}_{21} \equiv \gamma_{21} - i\delta_p$ for the ground state dephasing rate, and $\tilde{\gamma}_{31} = \Gamma/2 - i\Delta_p$ for practical EIT system.

From Eq. (11), one can find that the probe field has spatial dependence in transverse and longitudinal direction. However, the transverse dependence can be ignored for practical EIT experimental condition: (i) The beam width of probe beam is much smaller than that of coupling beam. $\sigma_{\text{probe}} \simeq 0.1\sigma$ for example. As we can see from Eq. (13), the term of $\exp(-\boldsymbol{\rho}^2/2\sigma^2\beta^2) \simeq 1$ when $|\boldsymbol{\rho}| \simeq 0.1\sigma$ and $\beta \geqslant 1$. Thus one can safely ignore $\boldsymbol{\rho}$ dependence of probe beam. (ii) The probe beam propagates on axis with the coupling beam. The probe beam is focused around $\boldsymbol{\rho} = 0$, which corresponds to the peak intensity of coupling beam. Hence, the function of Λ is symmetric to probe beam. If the propagation direction of the probe beam is off-axis, the probe beam can only see the local coupling beam intensity at $\boldsymbol{\rho} = \boldsymbol{\rho}_c \neq 0$. It doesn't affect the main physics of probe beam propagation. The more detailed calculations and simulations are given in the Appendix. In Fig. 2 we just compare the numerical results of the curvature and beam width of probe beam with respect to the case without having the term from atomic polarization Λ. The parameters are given by $\sigma = 1$ mm, $\sigma_{\text{probe}} = 0.2\sigma$, $L = 5$ cm, $\Delta_p = 0 =$
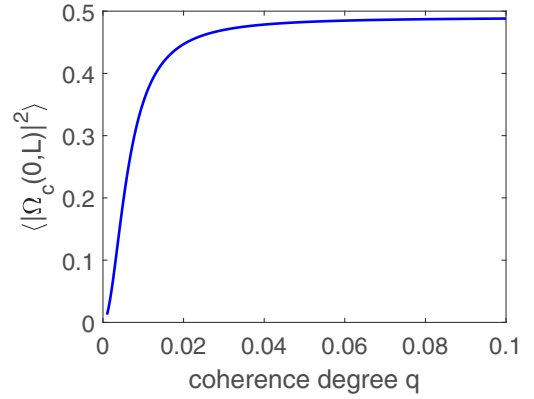

FIG. 3. The statistical average intensity of the coupling field in the center $\boldsymbol{\rho} = 0$ and at $z = L$ versus the global coherence degree q. The parameters we used here are $\Omega_0 = 0.7\Gamma$, $\Delta_p = 0 = \delta_p$, $\sigma = 1$ mm, $L = 5$ cm, and $k = 2\pi/\lambda$, with $\lambda = 780$ nm.

δ, $\Omega_0 = 0.7\Gamma$, $\lambda = 780$ nm, $\tau = 40(1/\Gamma)$, $\omega = (1/40)\Gamma$, and $q = 0.002$. Please note that we have use the upper limit in frequency according to $\omega\tau = 1$. As we can see, the curvature and the width of the probe beam are almost the same as those of the Gaussian beam propagating in free space when $\sigma_{\text{probe}} = 0.2\sigma$. When the probe beam width is getting smaller, the transverse distribution is closer to the distribution of the Gaussian beam with $\Lambda = 0$. This implies that the transverse variation is insignificant in the beam propagation.

After dropping the Laplacian term in Eq. (11), the solution of the probe field is

$$\tilde{\Omega}_p(z, \omega) = \tilde{\Omega}_p(0, \omega) \exp\left[-\int_0^z dz' \Lambda(z', \omega) \right], \quad (14)$$

where $\tilde{\Omega}_p(0, \omega) = (\Omega_{p0}\tau/\sqrt{2}) \exp(-\omega^2\tau^2/4)$ is the spectra of the input probe field, which is the Fourier transform of the input probe field in the time domain given by $\Omega_p(0, t) = \Omega_{p0} \exp(-t^2/\tau^2)$, in which Ω_{p0} is the peak value of the probe Rabi frequency and τ is the pulse width of the probe field.

Once the input probe field pulse $\Omega_p(0, t)$ is determined, we can find the output probe field pulse by the inverse Fourier transform of Eq. (14).

III. RESULTS AND DISCUSSIONS

In Sec. II, we have developed a theory to describe the probe field propagation in the EIT system with a spatially partially coherent coupling field. In Eq. (9), it implies that the statistical average intensity of the coupling field depends on not only the peak intensity Ω_0 but also the spatial coherence degree q. Thus, it provides us an opportunity to study the group delay of the probe beam with respect to the degree of spatial coherence.

In Fig. 3, we have shown the relation between the statistical average intensity of the output coupling field. We set $\boldsymbol{\rho} = 0$ where the probe and coupling beams are overlapped in their beam center. The peak value of $\Omega_0 = 0.7\Gamma$ and the resonance condition have been used, i.e., $\Delta_p = 0 = \delta_p$. As we can see, when the global coherence degree q is larger than 0.04, the statistical average intensity of the coupling field approaches
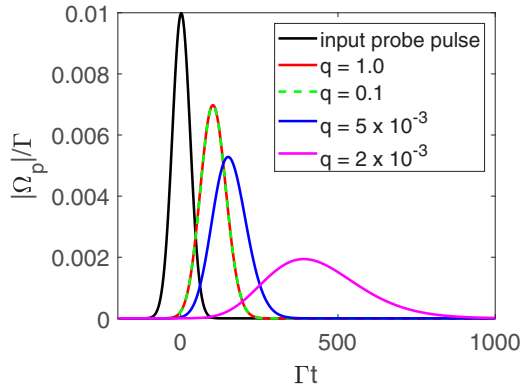
FIG. 4. The Rabi frequency of the probe field pulse $|\Omega_p|$ under various degrees of spatial coherence q. The black curve is the input probe pulse. The solid red, dashed green, solid blue, and solid magenta curves are the output pulses under the global spatial coherence degrees of $q = 1$, $q = 0.1$, $q = 5 \times 10^{-3}$, and $q = 2 \times 10^{-3}$, respectively. The input probe pulse is a Gaussian pulse with a pulse width of $\tau = 40(1/\Gamma)$. The optical density $\alpha = 50$, and $\gamma_{21} = 10^{-5}\Gamma$. Other parameters are the same as those in Fig. 3.

$|\Omega_0|^2$, which is the result of the fully coherent case. The statistical average intensity drops quickly when $q < 0.01$.

In order to have a clear visual picture of the relation of slow light and the spatial coherence degree, we have plotted the Rabi frequency of the input probe field pulse and the output probe pulse with different values of q in Fig. 4. The black curve represents the input probe pulse, which is the Gaussian pulse with a width of $\tau = 40/\Gamma$. The solid red, dashed green, solid blue, and solid magenta curves are the output probe pulse with values of $q = 1.0$, $q = 0.1$, $q = 5 \times 10^{-3}$, and $q = 2 \times 10^{-3}$, respectively. The optical density of the EIT medium is $\alpha = 50$, and the other parameters are the same as those in Fig. 3. The maximum of the Rabi frequency of the input probe pulse is 0.01Γ, which is much smaller than the Rabi frequency of the coupling field with the corresponding coherence degree. The low-intensity approximation in EIT is always satisfied in our theory. From Fig. 4, we can find that the group delay of the probe pulse is getting larger when the degree of spatial coherence is getting lower.

The group delay time of the probe pulse can be measured by the peak position between the input pulse and the output pulse [29]. In Fig. 4, we define the peak of the input probe pulse at $t = 0$; thus, it is easy to read the delay time of the output pulse. In Fig. 5, we have shown the ratio of the delay time between the partially coherent case and the fully coherent case, i.e., $T_D/T_{D,\text{coh}}$ with respect to the coherence degree q. As we can see, when the coherence degree $q > 0.01$, the delay time is closed to the delay time in the fully coherent case. However, when $q < 0.01$, the delay time increases significantly. The small range of q from 0 to 0.01 is zoomed-in in the inset in Fig. 5. It shows that the delay time can achieve about 10 times that of the fully coherent case when $q \simeq 10^{-3}$. There is clear evidence to show that, when $q = 0.002$, the value of $\beta^2 \simeq 10$, which means that the coupling beam intensity average decreases about 10 times, so that the group velocity of the probe field is 10 times slower because $v_g \propto 1/\langle|\Omega_c|^2\rangle$. Essentially, the enhancement of group delay under a spatially
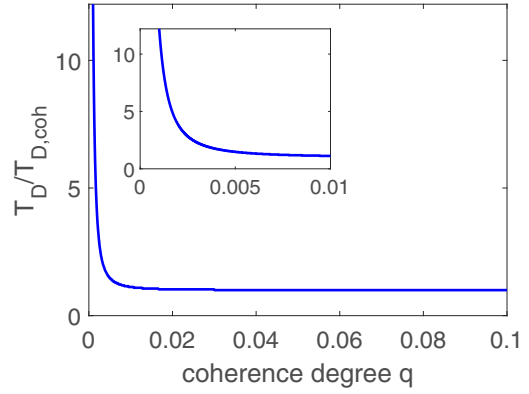

FIG. 5. The ratio of delay time $T_D/T_{D,\text{coh}}$ versus the coherence degree q. The range of q from 0 to 0.01 is zoomed-in in the inset.

partially coherent coupling field can be understood by the fact that the statistical average of the coupling field intensity is decreasing as the coherence degree is decreasing. The group velocity of the probe field pulse becomes smaller when the coupling field intensity decreases, so that we have a larger group delay time.

Finally, we discuss the Doppler-broadening effect, which is a practical phenomenon in EIT experiments using atomic vapors. The Doppler-broadening effect can be removed when one prepares the ultracold atoms by using the laser cooling technique, which is a mature technique in the field of atomic molecular and optical sciences. However, it is still an interesting issue in practical cases when the atomic ensembles are in room-temperature or even in hot atomic vapor systems. In a hot atomic vapor, the crucial problem is the Doppler shift. Fortunately, the problem can be resolved by the copropagation scheme, i.e., Ω_p and Ω_c propagate in the same direction [30,31]. For the case of the ^{87}Rb atom, the angular frequency difference between the two ground states $|1\rangle$ and $|2\rangle$ is $\omega_{21} = (E_1 - E_2)/\hbar = 2\pi \times 6.8$ GHz. In this copropagation setting, the two-photon detuning δ_D due to the Doppler shift of the root-mean-square atom velocity in the propagation direction of light, $\bar{v}$, is given by

$$\delta_D = |k_p - k_c|\bar{v} = \frac{\omega_{21}}{c}\bar{v}. \tag{15}$$

At the temperature of $100\,^{\circ}$C, $\delta_D \approx 2\pi \times 6$ kHz $= 0.001\Gamma$, which is less than the EIT linewidth $\Delta\omega_{\text{EIT}} \equiv |\Omega_c|^2/\Gamma$ in our case. However, when q is very small, such that $\beta^2 \geqslant \Omega_0^2/(\Gamma\delta_D)$, the Doppler shift is out of the EIT linewidth, and the Doppler broadening effect should be taken into account.

IV. CONCLUSION

In this work, we have studied the partial spatial coherence degree of the coupling field in the EIT system. We have pointed out that the statistical average of the coupling field intensity in the EIT medium is essentially dependent on the spatial coherence degree at input. Due to the decrement of the statistical average coupling field intensity at low coherence degree, the group delay time can be significantly enhanced. It can achieve about 10 times the group delay time of the fully coherent case when $q \simeq 10^{-3}$. This is a different mechanism

of the slow-light effect, and it is impossible to have an analog in the fully coherent case. In addition, we also discuss the Doppler-broadening effect in practical experiments, and we give the condition of the coherence degree to preserve the transparency of the EIT linewidth. The partial spatial coherences of interacting fields provide an extra degree of freedom in optical coherent atomic media like EIT, and it will open a different avenue to study atom-light interactions in the spatially partially coherent regime.

APPENDIX

In this Appendix, we try to find a solution of Eq. (11). As we know, when the term on the right-hand side vanishes, the fundamental mode of the probe beam is a Gaussian beam, which is the solution of the paraxial wave equation. Here we assume that the probe beam still maintains the Gaussian profile during the propagation when the term on the right-hand side is nonzero. We can use the trial solution given by

$$\tilde{\Omega}_p(r, z) = A \exp\left[ip(z) + \frac{ikr^2}{2q(z)}\right], \tag{A1}$$

where $p(z)$ and $q(z)$ are the two functions, which will be determined later. A is the given amplitude, which is a constant. $r = |\boldsymbol{\rho}| = \sqrt{x^2 + y^2}$ is the radial distance from the beam center at $(x, y) = (0, 0)$.

One can substitute Eq. (A1) into Eq. (11). Then one can obtain the following relation:

$$\left(\frac{1}{q(z)} + ip'(z)\right) + \frac{ikr^2}{2q^2(z)}[1 - q'(z)] + \Lambda(z, r) = 0, \tag{A2}$$

where Λ is the function given by Eq. (12).

In Eq. (12), we have the intensity profile of the coupling beam, which is the function of r and z, as shown in Eq. (13). As we have mentioned, the beam width of the probe beam is

much smaller than the coupling beam width, so that we can expand the exponent term of the coupling beam intensity to $O(r^2)$:

$$\langle|\Omega_c(r, z)|^2\rangle \simeq \frac{|\Omega_0|^2}{\beta^2}\left(1 - \frac{r^2}{2\sigma^2\beta^2}\right). \tag{A3}$$

After substituting Eq. (A3) into Eq. (12), one can expand Λ as follows:

$$\Lambda(z, r) \simeq \Lambda_0(z)r^0 + \Lambda_2(z)r^2, \tag{A4}$$

where

$$\Lambda_0(z) = \frac{(\Gamma\alpha/L)\beta^2(z)(\tilde{\gamma}_{12} - i\omega)}{D(z)} - i\frac{\omega}{c}, \tag{A5}$$

$$\Lambda_2(z) = \frac{(\Gamma\alpha/2L)(\tilde{\gamma}_{12} - i\omega)|\Omega_0|^2}{\sigma^2 D^2(z)}, \tag{A6}$$

where $D(z) \equiv 4\beta^2(z)(\tilde{\gamma}_{13} - i\omega)(\tilde{\gamma}_{12} - i\omega) + |\Omega_0|^2$.

Substituting Eq. (A4) into Eq. (A2) and collecting the order of r, we obtain

$$\left(\frac{1}{q(z)} + ip'(z) + \Lambda_0(z)\right)r^0$$
$$+ \left[\frac{ik}{2q^2(z)}[1 - q'(z)] + \Lambda_2(z)\right]r^2 = 0. \tag{A7}$$

From Eq. (A7), we have two equations for $q(z)$ and $p(z)$, which are

$$p'(z) - \frac{i}{q(z)} - i\Lambda_0(z) = 0, \tag{A8}$$

$$q'(z) + \frac{2i\Lambda_2(z)}{k}q^2(z) - 1 = 0. \tag{A9}$$

When $\Lambda_0 = 0 = \Lambda_2$, the solutions of $q(z)$ and $p(z)$ are

$$q(z) = z - iz_R, \tag{A10}$$

$$\exp[ip(z)] = \frac{w_0}{w(z)}\exp(i\psi), \tag{A11}$$

in which $z_R = \pi w_0^2/\lambda$ is the Rayleigh range of a Gaussian beam, and $\psi = \tan^{-1}(z/z_R)$ is the Gouy phase. w_0 is the beam waist of the Gaussian beam. $q(z)$ is related to the width $w(z)$ and the curvature $R(z)$ of the Gaussian beam, in which $R(z) = \text{Re}[q(z)^{-1}]^{-1}$ and $w^2(z) = (\lambda/\pi)\text{Im}[q(z)^{-1}]^{-1}$. When Λ_0 and Λ_2 are nonzero, one has to solve Eqs. (A8) and (A9). Since Λ_0 and Λ_2 are z dependent, it is difficult to obtain the analytical solutions of $q(z)$ and $p(z)$. We have shown the numerical calculation results of the beam curvature and the beam width in Fig. 2 in Sec. II.

[1] S. E. Harris, Phys. Today **50**(7), 36 (1997).

[2] M. Fleischhauer, A. Imamoglu, and J. P. Marangos, Rev. Mod. Phys. **77**, 633 (2005).

[3] G. S. Agarwal and S. Huang, Phys. Rev. A **81**, 041803(R) (2010).

[4] K.-H. Chiang and Y.-F. Chen, Phys. Rev. A **106**, 023707 (2022).

[5] K.-J. Boller, A. Imamoğlu, and S. E. Harris, Phys. Rev. Lett. **66**, 2593 (1991).

[6] S. E. Harris, J. E. Field, and A. Kasapi, Phys. Rev. A **46**, R29(R) (1992).

[7] L. V. Hau, S. E. Harris, Z. Dutton, and C. H. Behroozi, Nature (London) **397**, 594 (1999).

[8] D. F. Phillips, A. Fleischhauer, A. Mair, R. L. Walsworth, and M. D. Lukin, Phys. Rev. Lett. **86**, 783 (2001).

[9] C. Liu, Z. Dutton, C. H. Behroozi, and L. V. Hau, Nature (London) **409**, 490 (2001).

[10] L. Ma, O. Slattery, and X. Tang, J. Opt. **19**, 043001 (2017).

[11] D. Petrosyan, J. Otterbach, and M. Fleischhauer, Phys. Rev. Lett. **107**, 213601 (2011).

[12] Y.-L. Chuang, I. A. Yu, and R. K. Lee, Phys. Rev. A **91**, 063818 (2015).

[13] Y.-L. Chuang, R.-K. Lee, and I. A. Yu, Opt. Express **29**, 3928 (2021).

[14] R. E. Kinzly, J. Opt. Soc. Am. **62**, 386 (1972).

[15] S. C. Som, C. Delisle, and M. Drouin, Opt. Commun. **32**, 370 (1980).

[16] X. Ma and G. R. Arce, Opt. Express **16**, 20126 (2008).

[17] O. Korotkova, Opt. Commun. **281**, 2342 (2008).

[18] Y. Cai and S. Zhu, Opt. Lett. **29**, 2716 (2004).

[19] C. H. Gan, G. Gbur, and T. D. Visser, Phys. Rev. Lett. **98**, 043908 (2007).

[20] P. Barberis-Blostein and M. Bienert, Phys. Rev. Lett. **98**, 033602 (2007).

[21] Y.-F. Chen, Y.-M. Kao, W.-H. Lin, and I. A. Yu, Phys. Rev. A **74**, 063807 (2006).

[22] A. Peng, M. Johnsson, W. P. Bowen, P. K. Lam, H.-A. Bachor, and J. J. Hope, Phys. Rev. A **71**, 033809 (2005).

[23] R. Simon, E. C. G. Sudarshan, and N. Mukunda, Phys. Rev. A **31**, 2419 (1985).

[24] E. Giese, R. Fickler, W. Zhang, L. Chen, and R. W. Boyd, Phys. Scr. **93**, 084001 (2018).

[25] P. Sharma, N. K. Pathak, and B. Kanseri, Results Phys. **27**, 104506 (2021).

[26] H. Defienne and S. Gigan, Phys. Rev. A **99**, 053831 (2019).

[27] Y. Ismail, S. Joshi, and F. Petruccione, Sci. Rep. **7**, 12091 (2017).

[28] Q. Y. Ismail, S. Joshi, and F. Petruccione, Proc. SPIE **9996**, 999601 (2016).

[29] Y.-W. Cho and Y.-H. Kim, Phys. Rev. A **82**, 033830 (2010).

[30] C.-Y. Hsu, Y.-S. Wang, J.-M. Chen, F.-C. Huang, Y.-T. Ke, E. K. Huang, W. Hung, K.-L. Chao, S.-S. Hsiao, Y.-H. Chen, C.-S. Chuu, Y.-C. Chen, Y.-F. Chen, and I. A. Yu, Opt. Express **29**, 4632 (2021).

[31] J.-M. Chen, C.-Y. Hsu, W.-K. Huang, S.-S. Hsiao, F.-C. Huang, Y.-H. Chen, C.-S. Chuu, Y.-C. Chen, Y.-F. Chen, and I. A. Yu, Phys. Rev. Res. **4**, 023132 (2022).